Tribology Online
Japanese Society of Tribologists

Tribology Online, 10, 5 (2015) 336-343.
ISSN 1881-2198
DOI 10.2474/trol.10.336

Article

Theoretical Evaluation of the Operational Characteristics in a Large Thrust Bearing

Duriseti Srikanth[1)*], Kaushal Chaturvedi[2)] and Chenna Kesava Reddy[3)]

[1)]Mechanical Engineering, MLRIT, Laxma Reddy Avenue
Dundigal, Hyderabad- 50043, India
[2)]BHEL, Corporate R&D
Adhoiwala, Dehradun-248001, India
[3)]Mechanical Engineering, JNTUH
Kukatpally, Hyderabad-500085, India
[*]Corresponding author: dvsrikanth1@hotmail.com

(Manuscript received 21 March 2014; accepted 1 December 2014; published 15 November 2015)
(Presented at ASIATRIB-2014, Agra, India, February 2014)

In this paper the non-dimensional load, volumetric flow rate, energy flux, oil film temperature and power loss parameters of a tilting-pad thrust bearing are formulated. The objective of the paper is to determine the novel non dimensional thermal, volumetric and power loss parameters in addition to the load and energy flux parameters of the bearing. The computation is done by formulating and numerically solving for the oil film thickness, two dimensional Reynolds', Vogel-Cameron viscosity-temperature relationship and energy equations at the different nodes of the oil film using a finite difference procedure. The planar film shape polynomial ensures the accuracy of the slider bearing shape and pressure distribution. The numerical procedure evaluates the value of '*a*' at which the load is maximum. The variation of the bearing centre of pressure with respect to the corresponding values of '*a*' is studied. From the fluid film temperature equation the rise in bearing temperature corresponding to the range of '*a*' values is determined. The oil film temperature distribution results are found satisfactory in terms of computer time and convergence criteria. The accuracy of the results is validated in the variation of the load and thermal contours. A mesh independence test is conducted using three meshes of different sizes. The mesh independent solution and convergence is obtained for the smallest mesh that also reduces simulation run time. This data and analysis serves as an input to determine the dynamic stiffness and damping coefficients. It includes the scope to develop a design method for safe operation of the bearing at any speeds in vertical hydro-electric rotors.

Keywords: non-dimensional, convergence, thermal, load, flow rate, power loss

1. Introduction

The present work encompasses the first stage of research activity aimed at understanding the phenomena involved in the working of a large tilting-pad thrust bearing. The thrust segment enables change of the oil film geometry and maintains its optimum shape, even with a changing load. The principle of a thrust pad bearing is based on a convergent wedge which is formed between two surfaces in relative motion. The oil film shape equation for a flat sector-shaped bearing surface is formulated. Two dimensional Reynolds' equation is also formulated for this bearing. The energy equation governing the generation and transfer of heat is coupled and solved with the Reynolds' equation. The aim of this paper is to formulate and determine the non-dimensional load and thermal parameters as functions of the film shape parameter. Here the variations of the above parameters are plotted for a given range of film shape parameter values and L/B ratios without considering pad deformation. This helps in determining the values of a and L/B ratio for which the above parameters are maximum. And also enables better bearing design. Also a mesh independence test is conducted using three sizes of meshes to obtain a mesh independent solution and convergence.

Load capacity, film thickness, stiffness, damping coefficients and temperature are parameters to be determined first in the design of thrust bearings compatible with given operating conditions. This analysis was illustrated by Chu [1] using a matrix inversion method to develop an algorithm for designing

Copyright © 2015 Japanese Society of Tribologists

the optimum shape and pressure distribution of a slider bearing. An understanding of the oil film shape and an improved computation method are needed to predict performance and design of such bearings.

Modified numerical solutions are required to determine the pressure, temperature and elastic deformation of the oil film and pad respectively using three dimensional flow. Yang and Rodkiewicz [2] used a finite difference method to determine the thermo elasto-hydrodynamic lubrication of a tilting pad. A finite difference method was used to determine the pressure, temperature and elastic deformation of the oil film and pad respectively. Sinha et al. [3] provided a realistic simulation for the pressure distribution by solving the Reynolds' equation for a large thrust bearing. The film thickness was unknown and the centre of pressure was known together with the energy and bending equations. The resultant film shape of the thrust pad was determined by a thermo-elastic analysis. Experimental and theoretical investigations into the effect of oil thermal properties on the functioning of a tilting pad thrust bearing using polyolefin oil, ester and mineral oil were carried out. Glavatskih et al. [4] analyzed this data in terms of inlet and outlet film thickness, bearing operating temperature and power loss.

Finite element methods to analyze the performance of hydrodynamic tilting pad thrust bearings are very useful and have gained importance. Markin et al. [5] compared the results of this method satisfactorily with experimental data obtained on spherical pivoted pads. Comparison of performance in PTFE and babbit bearings of nominally same area reveal that the power losses are identical. Ettles et al. [6] found in conformity the software and experimental predictions of these bearings. Tests conducted on two bearings for influence of the pad facing material on the film thicknesses and pad temperatures revealed certain differences and similarities. Mc Carthy et al. [7] conducted the experiments for two bearings one with white metal and the other with a PTFE layer. Sensors were mounted on the pads to monitor the frictional torque, film thicknesses and temperatures. Oil film thicknesses differed but there was no significant temperature differences in the two bearings.

A numerical procedure to analyse wavy thrust bearings assuming two circular rotating discs relative to each other was developed. A Reynolds' equation based procedure that simulated wavy geometries that get worn out during starts and stops and bearing loading conditions was formulated by Zhao et al [8]. Each of the nine linear stiffness and damping coefficients were calculated using a three degrees of freedom system. The eigen values of the system using these linear coefficients were obtained by solving the homogeneous equations of motion. The stability of the bearing system was expressed in terms of the logarithmic decrement obtained from these eigen values. In the transient thermo hydrodynamic lubrication of bearings the decrease of film thickness caused by enhancing load made the film temperature rise gradually. Li and Qing [9] derived the equations of film thickness, pressure and temperature in thrust bearings with tilting pads. Glavatskih and Fillon [10] presented a TEHD analysis of thrust bearings with PTFE faced pads. The effect of pad active face geometry on temperature, film thickness and pressure profile were investigated.

Hydrodynamic principles were used in the design of tilting pad bearings utilized in mechanisms carrying shaft thrust loads. Ni et al. [11] optimized the pivot positions of such tilting pad thrust bearings. The effects of elastic deformation of pad surface, rotational speed, axial load and oil viscosity grade on tilting pad thrust bearing performance using the TEHD lubrication model were analyzed. Jiang et al showed that the maximum pressure was reduced and the minimum film thickness was decreased when pad deformation was taken into account.

A finite element method was used to predict the TEHD behavior of the Three Gorges hydro generator bearing. Zhong-De and Hong [12] showed that the agreement between the real time and theoretical operational parameters was good.

2. Governing equations'

a) In hydrodynamic pressure generation an oil film requires that its film thickness decrease within the film length in the direction of sliding. The form of reduction of the film thickness is less important than its magnitude. Convergence is achieved by machining the appropriate profile on the face of a tilting pad thrust bearing. For limited combinations of load and speed the optimum film ratio is obtained for only one value of minimum film thickness. For all operating conditions an optimally located pivot ensures optimum performance. Equation for the non-dimensional thickness of the oil film with reference to Etsion [13] is:

$$\begin{aligned} H &= h / h_o \\ &= 1 + \left(ar_{cp} / B\right)\tan\left(\beta - \theta_{cp}\right) - \left(ar / B\right)\sin\left(\theta - \theta_{cp}\right) \\ &+ \left[\left(a / B\right) r_{cp}\tan\left(\beta - \theta_{cp}\right) - \gamma / L\right] \\ &\times \left[r\cos\left(\theta - \theta_{cp}\right) - r_{cp}\right] \end{aligned} \tag{1}$$

b) The Reynolds' equation is obtained by introducing the lowest order terms of the Navier-Stokes equation in the continuity equation which is then integrated across the film. The analysis of hydrodynamic thrust bearings is based on Reynolds' equation for the pressure distribution. Values of viscosity, specific heat etc. obtained from the temperature field in the oil film are substituted in the Reynolds' equation, to determine the pressure field. In load estimation the pressure at the edges is made zero to suit realistic conditions. The Reynolds' equation in non-dimensional form for a sector-shaped thrust segment and incompressible lubricant referred in Srikanth et al. [14] under steady state condition is

$$\frac{\partial^2}{\partial R^2}\left[\frac{RH^3P}{\bar{\mu}}\right]+\frac{RH^3}{\bar{\mu}}\frac{\partial^2 P}{\partial R^2}$$
$$-P\frac{\partial^2}{\partial R^2}\left[\frac{RH^3}{\bar{\mu}}\right]+\frac{1}{R\beta^2}\frac{\partial^2}{\partial\bar{\theta}^2}\left[\frac{H^3P}{\bar{\mu}}\right] \quad (2)$$
$$+\frac{1}{R\beta^2}\frac{H^3}{\bar{\mu}}\frac{\partial^2 P}{\partial\bar{\theta}^2}-\frac{P}{R\beta^2}\frac{\partial^2}{\partial\bar{\theta}^2}\left[\frac{H^3}{\bar{\mu}}\right]$$
$$=12R\frac{\partial H}{\partial\theta}+24R\beta V$$

The boundary conditions associated with the Reynolds' equation for the nodes lying on the boundary are

$$P=0 \quad \text{at} \quad r=r_i, r=r_o, \theta=0, \theta=\beta. \quad (3)$$

c) Thermal effects caused due to viscous shearing of lubricant layers limit performance in a number of ways. The generation of heat lowers the effective film viscosity, resulting in the decreased load capacity. The flow of oil transports this heat to other parts of the film. The energy equation governs this heat generation and transport. The pressures and temperatures are formulated in terms of finite differences. The conduction of heat to the runner and segment surfaces are neglected. This is because the runner is exposed to the varying temperature of the oil film. The oil moves across the gap between the pads and then from the leading edge to the trailing edge. The thermal inertia of the runner prevents it from assuming the oil temperature instantaneously. Thus the temperature of the runner along its periphery varies much less than the temperature in the stationary parts. Hence the temperature of the runner varies by less than 1°C and the temperature along the thrust pad rises by 15°C to 20°C. The energy equation for laminar flow and an incompressible lubricant is

$$C_p\rho\left[q_r\frac{\partial T}{\partial r}+q_\theta\frac{1}{r}\frac{\partial T}{\partial\theta}\right]=\dot{E} \quad (4)$$

The radial flow is given by

$$q_r=-\frac{h^3}{12\mu}\frac{\partial p}{\partial r} \quad (5)$$

and circumferential flow is

$$q_\theta=\frac{r\omega h}{2}-\frac{h^3}{12\mu}\frac{1}{r}\frac{\partial p}{\partial\theta} \quad (6)$$

The energy eq. (4) is re-written as

$$\dot{E}=\frac{\mu}{h}(\omega r)^2+\frac{h^3}{12\mu}\left[\left(\frac{1}{r}\frac{\partial p}{\partial\theta}\right)^2+\left(\frac{\partial p}{\partial r}\right)^2\right] \quad (7)$$

The non-dimensional form of the energy equation referred in Chaturvedi et al. [15] is

$$\frac{\partial T}{\partial\theta}\left[nH^2-\frac{H^4}{12R^2}\left(\frac{L}{R_o}\right)^2\left(\frac{\partial P}{\partial\theta}\right)\right]-\frac{H^4}{12}\left(\frac{L}{R_o}\right)^2\left(\frac{\partial P}{\partial R}\right)\left(\frac{\partial T}{\partial R}\right)$$
$$=4n^2R^2+\left(\frac{L}{R_o}\right)^4\frac{H^4}{12}\left[\left(\frac{\partial P}{\partial R}\right)^2+\frac{1}{R^2}\left(\frac{\partial P}{\partial\theta}\right)^2\right]$$

The Vogel-Cameron equation (9) shows the variation of viscosity with temperature and is introduced in the iterative process.

$$\mu=\mu_0 e^{A/(T+95)} \quad (9)$$

d) The hot oil carryover effect investigated by Ettles [16] is considered in determining the inlet and outlet temperatures in a single sweep. The lubricant entering the wedge at the inlet edge is heated to some extent by the hot runner. In the inter-pad space this lubricant also consists of some oil in the preceding pad and some oil from the bath to make up for the oil lost due to side leakage. Thus, the actual inlet temperature in the oil film is higher than the bulk oil temperature.

The hot oil carry over effect is represented as

$$T_{out}=T_{\sup}+\Delta T\left(\frac{2-k}{2-2k}\right) \quad (10)$$

where $$k=\frac{T_{in}-T_{\sup p}}{T_{run}-T_{\sup p}} \quad (11)$$

k is assumed to be = 0.83 in our study

$$T_{in}=T_{out}-\Delta T \quad (12)$$

Thus once the temperature of the bulk oil in the housing is known and temperature rise has been calculated, the inlet temperature, the outlet temperature and the runner temperature can be calculated.

3. Computational procedure

The governing equation for hydrodynamic lubrication, i.e. Reynolds' equation is solved for a laminar, flow regime. Solution of the Reynolds' equation using a finite difference discretization of the thrust pad is obtained considering a total of 81 nodes as in Fig. 1. The truncated Taylor series expansion for three successive grid points is applied for approximating the derivatives in the differential equation and in formulating the Reynolds' finite difference equation. The central difference form is used to determine functional values at adjacent nodes on either side in order to evaluate the required derivatives in the interior. The forward or backward difference form is used when the node is on the leading or trailing edge or inner or outer radius. The finite difference form of the Reynolds' equation is written for every node and a resultant set of simultaneous linear algebraic equations

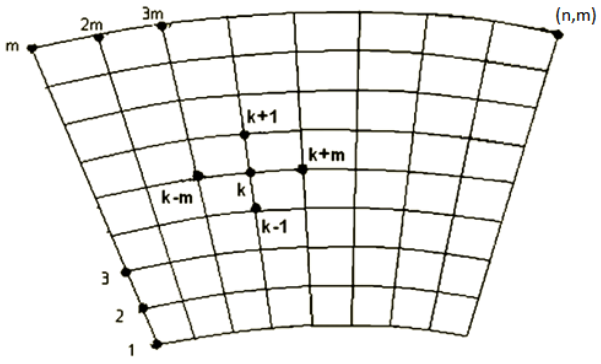

Fig. 1 Discretization of pad

Table 1 Thrust Bearing Geometry

Bearing Dimensions	**Authors' data**	**Jiangs' data**
Outer Diameter (m)	1.275	2.2
Inner Diameter (m)	0.75	1.565
Pad thickness (mm)	40	100
Groove width (mm)	84	100
Trailing edge film thickness (μm)	52.6	63.6
Operating Conditions		
Load (MN)	4	5
Rotational speed (rads/s)	14.28	9
Oil pot temperature (°C)	40	45
Oil Properties		
ISO VGgrade	46	32
γ (cSt) at 40°C	46	32
γ (cSt) at 100°C	6.72	5.3
ρ (g/m^3) at 15°C	0.875	0.870

obtained are solved by matrix inversion.

The energy equation that governs the generation of heat and transport is solved simultaneously using the same finite difference method and pad discretization. The initial temperature values at the leading edge are specified so that the successive values of the downstream temperature are computed in the flow direction. The use of either the forward, central or backward difference form of the Taylor series expansion is made depending on the position of the node. The oil pressure and temperature used in the determination of the non-dimensional load and thermal parameters pertain to the authors' input data listed in Table 1.

4. Non dimensional load, centre of pressure and maximum temperature

In terms of the oil film shape parameter 'a' the non-dimensional load parameter, centre of pressure and fluid film temperature with reference to Chaturvedi [17] are described as follows.

$$\bar{W} = \frac{Wh_o}{6\mu UB^2 L} = \frac{1}{a}\left[\ln(1+a)\frac{1}{a} - \frac{2}{(a+2)}\right] \tag{13}$$

$$\bar{X}_{cp} = \frac{\left[2(1+a)\ln(1+a)(1+\frac{3}{a}) - (5a+6)\right]}{2\left[\ln(1+a)(a+2) - 2a\right]} \tag{14}$$

$$\bar{T}_B = \frac{\frac{1}{a}\left[2\left(\frac{a+2}{a+1}\right)\ln(1+a) - 3\left(\frac{a}{a+1}\right)\right]}{\left[\frac{1}{a^2}\ln(1+a) - \frac{1}{a}\frac{2}{(a+2)}\right]} \tag{15}$$

5. Non dimensional thermal parameters

Similarly the non-dimensional volume flow rate $\bar{Q}$ is given as

$$\bar{Q} = \frac{Q_x}{Uh_o L} \tag{16}$$

The non-dimensional energy flux rate $\bar{E}$, oil film temperature $\bar{T}$ and power loss E_{pl} are represented as

$$\bar{E} = \frac{Eh_o}{\mu U^2 BL} \tag{17}$$

$$\bar{T} = \frac{3T\rho C_p BL}{2W} \tag{18}$$

$$E_{pl} = \frac{E\sqrt{3/2}}{\mu^{1/2}U^{1/2}W^{1/2}B^{1/2}L^{1/2}} \tag{19}$$

6. Results and discussions

a) Figures 2 and 3 show the pressure distributions pertaining to the set of the author and Jiangs' et al. [18] data listed in Table 1. The x and y axes represent the respective coordinates of a point on the pad. The y-axes

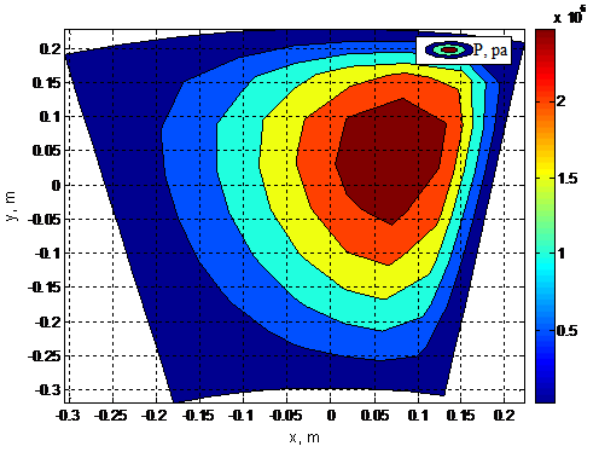

Fig. 2 Film pressure distribution in a flat pad, authors' data

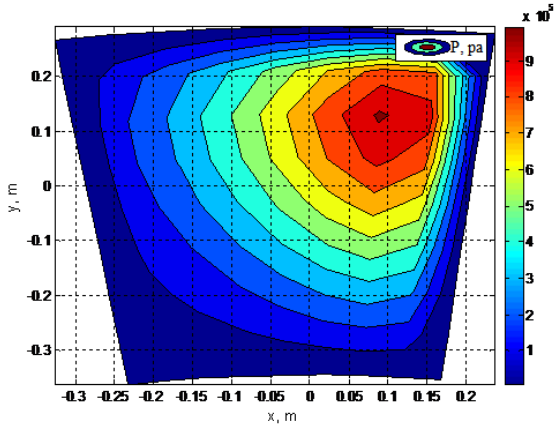

Fig. 3 Film pressure distribution in a flat pad, Jiangs' data

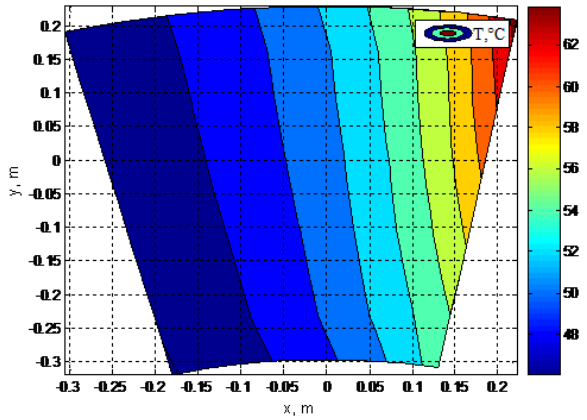

Fig. 4 Film temperature distribution of a flat pad, authors' data

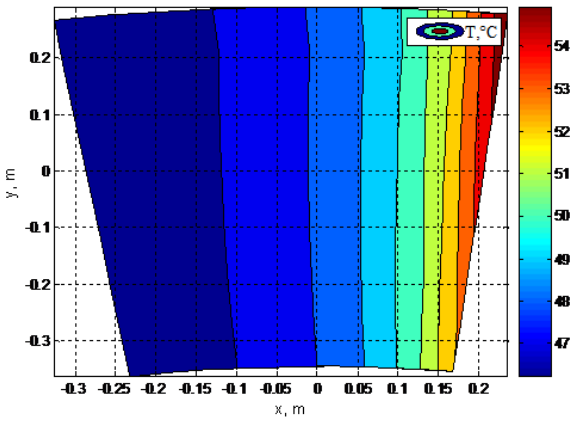

Fig. 5 Film temperature distribution of a flat pad, Jiangs' data

acts along the vertical radius and the origin of this coordinate axes is located at the centre of pressure. This data pertains to large tilting pad thrust bearings used to support vertical hydroelectric generators. The numerical accuracy of the pressure distribution ensures the 0.1 percent convergence limit. The maximum pressures of the two cases are 2.9792 MPa and 1.01 MPa respectively.

b) The viscosity of the supply oil is different from that of the oil entering the load carrying film. The temperature variation across the thickness of the oil film is neglected. The occurrence of reverse flow in the inlet region makes obtaining a solution using initial values difficult. The temperature distribution in the oil film for the authors' and Jiangs' data are shown in Figs. 4 and 5. The maximum temperature is located at the outer radius and corner of the trailing edge. The temperature contours near the trailing edge and the inner radius are bent forward, which indicates less temperature rise. The temperature variation along the left half of the pad is less when compared to the right half. The maximum temperature values for the authors' and Jiangs' data are

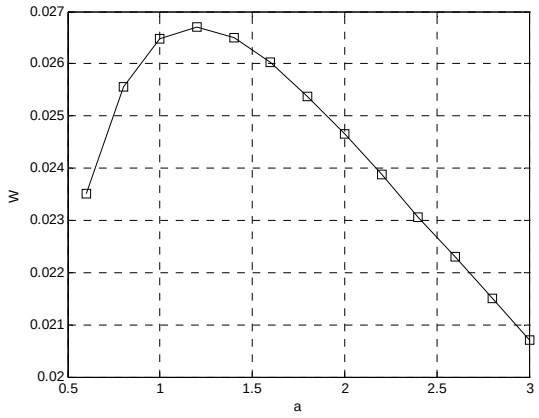

Fig. 6 Variation of load carrying capacity '$\overline{W}$' with oil film shape parameter 'a'

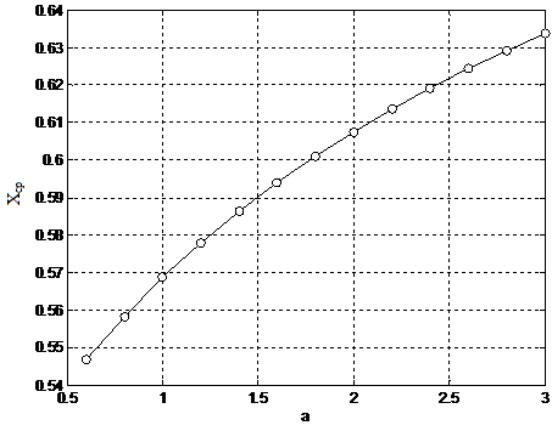

Fig. 7 Variation of centre of pressure with oil film shape parameter 'a'

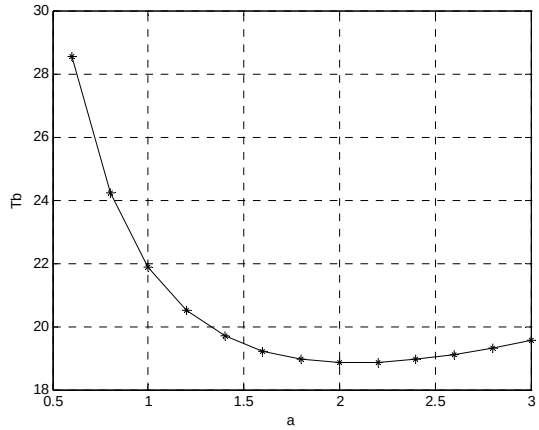

Fig. 8 Variation of bearing temperature with oil film shape parameter 'a'

64.6°C and 55.9°C. The pressure and temperature values are not in agreement because pad deformation has been considered only in the case of Jiangs' data.

c) The ratio of the difference between the inlet and outlet film thicknesses to the outlet film thickness is the

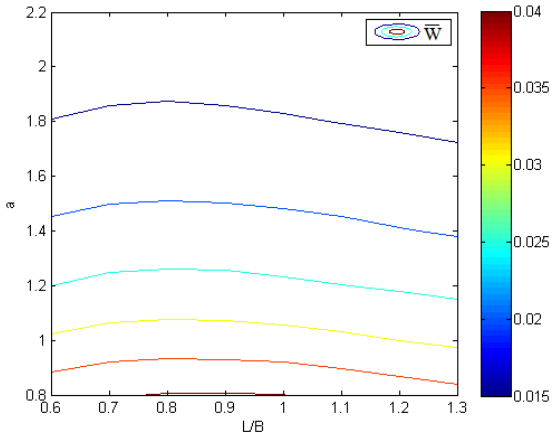

Fig. 9 Non dimensional load $\bar{W}$ to film parameter a and L/B

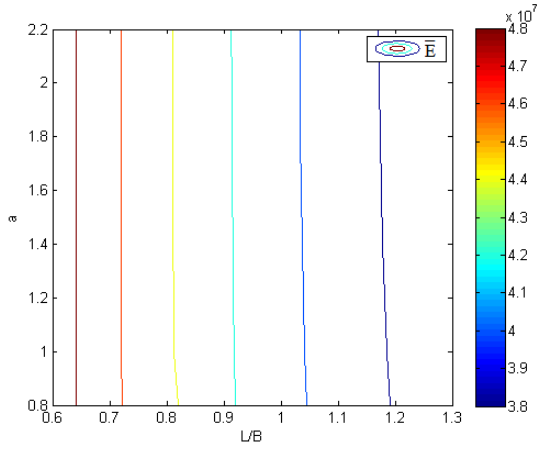

Fig. 11 Non dimensional energy flux $\bar{E}$ to film parameter 'a' and L/B

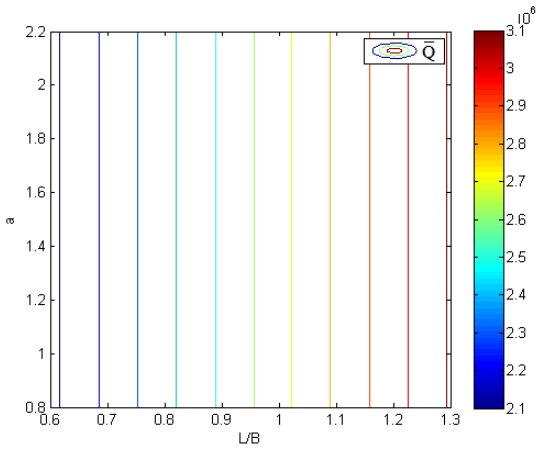

Fig. 10 Non dimensional volume flow rate to film parameter a and L/B

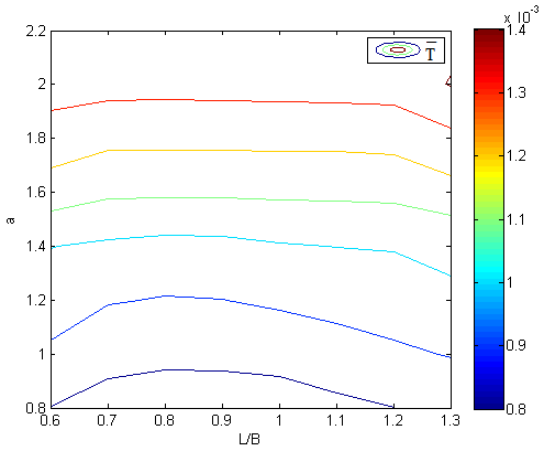

Fig. 12 Non dimensional film temperature to film parameter a and L/B

film shape parameter, denoted by 'a'. The aim is to find the value of 'a' at which the bearing load is maximum. This is done by substituting the values of 'a' ranging from 0.6 to 3.0 in the eq. (13). Figure 6 shows the variation of '$\bar{W}$' with 'a'. It is found that the maximum load occurs at the value of a = 1.2. The total load on the bearing gradually increases for 'a' values from 0 to 1.2 and then drops for 1.4 to 2.4. The centre of pressures for the different values of 'a' from 0.6 to 3.0 are obtained by substitution in eq. (14). Figure 7 shows the variation of $\bar{X}_{cp}$ with a. The corresponding value of $\bar{X}_{cp}$ for maximum load is 0.5779. Figure 8 shows the variation of $\bar{T}_B$ with a. The minimum rise in the bearing temperature occurs at the value of 'a' equal to 2.0. This corresponding location of the centre of pressure is at 0.6074.

d) The accuracy of the numerical analysis is verified in terms of the magnitude of the non-dimensional parameters obtained for the given range. The contours of the parameters are plotted for 'a' ranging from 0.6 to 1.3 and 'L/B' ratio from 0.8 to 2.2. The value of non-dimensional load $\bar{W}$ at a = 0.8 and 'L/B' = 0.6 is 0.0381 and decreases to 0.0105 for a = 2.2 and 'L/B' = 1.3 as shown in Fig. 9. The non-dimensional volume flow rate $\bar{Q}$ plotted for the given range of 'a' and 'L/B' values results in parallel vertical contours as shown in Fig. 10. The value of $\bar{Q}$ at a = 0.8 and 'L/B' = 0.6 is 2.075e+6 and increases to 3.1109e+6 at a = 2.2 and 'L/B' = 1.3. As shown in Fig. 11 vertical contours of non-dimensional energy flux $\bar{E}$ decrease from 4.9081e+7 to 3.6355e+7. The contour values for non-dimensional temperature increase from 0.0008 to 0.0014 in the considered range as in Fig. 12. The required non-dimensional power loss contours are obtained as shown in Fig. 13. These non-dimensional power loss values increase as shown from 1e+6 to 1.8e+6.

e) The aim is to have a unique solution wherein the simulated output values of integrated load, R_{cp} and θ_{cp} converge to a steady specified values corresponding to a pressure distribution with maximum nodal pressure of 4.5 MPa.

Although the solution satisfies the convergence based on load and centre of pressure location values, it has to be

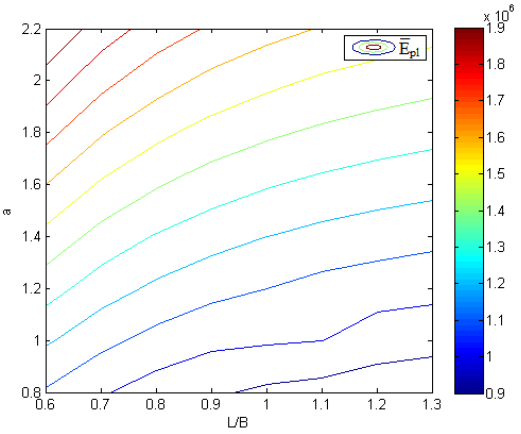

Fig. 13 Non dimensional power loss E_{pl} to film parameter a and L/B

made sure that the solution is also independent of the mesh resolution. This check is carried out once to determine right sizing of mesh. This analysis improves the validity of the results. The mesh independence study is straight forward and done as follows.

1. The initial simulation is run with a 9 × 9 nodal mesh and the load, R_{cp} and θ_{cp} values are found to be 2.1663e^6, 1.0557 m and 0.2575 radians.
2. The mesh is refined taking a 10 × 10 nodal matrix and the values obtained for load, R_{cp} and θ_{cp} are 2.0957e^6 , 1.0565m and 0.2603 radians.

These are not the same as obtained for the 9 × 9 mesh and have also not converged to our prescribed values. This shows that the solution is changing because of the mesh resolution and hence it is not yet independent of the mesh. The mesh is refined further to a 11 × 11 nodal matrix which yields values of load, R_{cp} and θ_{cp} of 2.057 e^6, 1.0571 m and 0.2625 radians. The values of the 9 × 9 nodal matrix converge within ± 1% of our earlier prescribed values for 4.5 MPa maximum nodal pressure distribution. This gives the mesh independent solution and is obtained by using the smallest mesh that reduces the simulation run time.

7. Conclusion

The modified Reynolds' and energy equations are solved simultaneously using a computer aided numerical model for the film pressure and temperature distributions. The model accounts for variations in the viscosity and the hot oil carry over effect. The variation of load, centre of pressure and temperature with 'a' are plotted and analyzed. The maximum load and minimum rise of bearing temperature occur at a = 1.2 and a = 2.0 respectively. It is inferred from the above contours that for an increase in 'a' and 'L/B' ratio, the values of non-dimensional load and energy flux decrease whereas volume flow rate and power loss increase. The values of 'a' and 'L/B' for maximum bearing load and minimum temperature, power loss are determined. Lack of agreement between the pressure and temperature distributions pertaining to the authors' and Jiangs' data is because pad deformation has been considered in the laters' case only. The linear objective film shape polynomial is easy to analyse in conjunction with the Reynolds' equation. The advantage of this equation is that it satisfies the requirement of flatness of the thrust segment and permits tilt in both directions. It thereby ensures accuracy of the slider bearing shape and pressure distribution. In view of the integrated plot function in the program the computer time per plot is minimal at approx. 3 secs. The mesh independent solution is obtained using the smallest 9 × 9 mesh that reduces simulation time. This theoretical data is useful in comparison with the actual data obtained by conducting experimental measurements of vertical machine rotors.

Nomenclature

a	it is the ratio of the difference between inlet and outlet film thickness to the outlet film thickness, $(h_o - h_i)/ h_o$
h	oil film thickness , m
h_o	oil film thickness at the trailing edge, m
p	pressure in the oil film , Pa
q_r	flow in the radial direction per unit length, m^2/s
q_θ	flow in th e circumferential direction per unit length, m^2/s.
r	radial coordinate of the runner, m.
t	transit time, B/U, s
A	constant for calculating viscosity, °C
B	circumferential length of the thrust segment, m
C_P	specific. heat at constant pressure, kcal/kg°C.
D_i	inner diameter of the thrust bearing, m
D_o	outer diameter of the thrust bearing, m
$\dot{E}$	heat dissipation rate in the oil film, per unit area, W/m^2
$\bar{E}$	non dimensional energy flux rate
H	non-dimensional thickness of the oil film, h/h_o
L	radial length of the thrust pad, m
N	angular speed of the runner, rpm
P	non-dimensional pressure
$\bar{Q}$	non dimensional volume flow rate
R	radius of the runner, m
R_i	inner radius of the pad, m
R_o	outer radius of the pad, m.
T	non-dimensional oil film temperature.
U, V	velocity along and normal to surface, m/s
W	load on bearing, N
$\bar{W}$	non dimensional load parameter.
X	x-cordinate of a point, m
Y	y-cordinate of a point, m
X_{cp}	centre of pressure, m
Z	number of pads
β	angular extent of the thrust pad, radians.
E_{pl}	non dimensional load parameter
γ	film thickness ratio

μ viscosity of oil , Pa·s
$\bar{\mu}$ non-dimensional viscosity
θ angle from the leading edge, rad
θ_{cp} angular location of the centre of pressure, rad
ρ density of oil, kg/m^3
ω :angular speed of the runner, rad/s

References

[1] Chu, H., "Shape Optimum Design of Slider Bearings Using Inverse Methods," Tribology International, 40, 5, 2007, 906-914.

[2] Yang, P. and Rodkiewicz, C. M., "On the Numerical Analysis to the Thermoelastohydrodynamic Lubrication of a Tilting Pad Inclusive of Side Leakage," Tribology Transactions, 40, 2, 1997, 259-266.

[3] Sinha, A. N., Athre, K. and Biswas, S., "Non-Linear Solution of Reynolds Equation for Thermoelastohydrodynamic Analysis of Thrust Pad Bearing," Industrial Lubrication and Tribology, 53, 5, 2001, 202-210.

[4] Glavatskih, S. B., Fillon, M. and Larsson, R., "The Significance of Oil Thermal Properties on the Performance of a Tilting-Pad Thrust Bearing," Transactions of the ASME, Journal of Tribology, 124, 2, 2001, 377-385.

[5] Markin, D., McCarthy, D. M. C. and Glavatskih, S. B., "A FEM Approach to Simulation of Tilting-Pad Thrust Bearing Assemblies," Tribology International, 36, 11, 2003, 807-814.

[6] Ettles, C. M. M., Knox, R. T., Ferguson, J. H. and Horner, D., "Test Results for PTFE-Faced Thrust Pads with Direct Comparison Against Babbitt Faced Pads and Correlation with Analysis," Transactions of the ASME, Journal of Tribology, 125, 4, 2003, 814-824.

[7] McCarthy, D. M. C., Glavatskih, S. B. and Sherrington, I., "Oil-Film Thickness and Temperature Measurements in PTFE and Babbitt Faced Tilting-Pad Thrust Bearings," Proceedings of the Institution of Mechanical Engineers, Part J: Journal of Engineering Tribology, 219, 3, 2005, 179-185.

[8] Zhao, H., Choy. F. K. and Braun, M. J., "Dynamic Characteristics and Stability Analysis of a Wavy Thrust Bearing," Tribology Transactions, 48, 1, 2005, 133-139.

[9] Zhong, L. and Tong, Q., "Study on Transient Lubrication Performance of Thrust Bearings with Tilting Pads Set on Variation load," Zhongguo Jixie Gongcheng/China Mechanical Engineering, 15, 2004, 1326-1328.

[10] Fillon, M. and Glavatskih, S. B., "PTFE-Faced Centre Pivot Thrust Pad Bearings: Factors Affecting TEHD Performance," Tribology International, 41, 12, 2008, 1219-1225.

[11] Ni, W., Griffiths, C., Bartholme, D. and Hergert, R., "Two Dimensional Analytical Analysis of Fluid Film Thickness on Pivoted Tilting Pad Bearings," Powertran and Fluid Systems, Conferences and Exhibitions, October, Chicago, 2007, USA.

[12] Zhong-de, W. and Hong, Z., "Performance Analysis of Thrust Bearing for Three Gorges Generator," Large Electric Machine and Hydraulic Turbine, 2011, 2, 9.

[13] Etsion, I., "Design Charts for Arbitrarily-Pivoted, Liquid-Lubricated, Flat-Sector-Pad Thrust Bearing", Transactions of the ASME, Journal of Lubrication Technology, 100, 2, 1978, 279-286.

[14] Srikanth, D. V., Chaturvedi, K. K. and Reddy, A. C. K., "Modelling of Large Tilting Pad Thrust Bearing Stiffness and Damping Coefficients," Tribology in Industry, 31, 3-4, 2009, 23-28

[15] Chaturvedi, K. K., Athre. K., Nath, Y. and Biswas, S., "Refinement in Estimation of Load Capacity and Temperature Distribution of Pad Bearings," Proceedings of Eurotrib, 1989.

[16] Ettles, C., "Hot Oil Carry Over in Thrust Bearings," Proceedings of the Institution of Mechanical Engineers, 184, 12, 1969, 75-81.

[17] Chaturvedi, K. K., "Deformation and Heat Transfer Effects in Conventional and Water - Cooled Spring - Supported Tilting - Pad Thrust Bearings," Industrial Tribology, Machine Dynamics and Maintenance Centre, IIT Delhi, 1994.

[18] Jiang, X., Wang, J. and Fang, J., "Thermal Elastohydrodynamic Lubrication Analysis of Tilting Pad Thrust Bearings," Journal of Engineering Tribology, 225, 2, 2011, 51-57.